CHEMISTRY
A EUROPEAN JOURNAL

DOI: 10.1002/chem.200601457

Effect of Electron Donors on the Radical Polymerization of Vinyl Acetate Mediated by [Co(acac)$_2$]: Degenerative Transfer versus Reversible Homolytic Cleavage of an Organocobalt(III) Complex

Sébastien Maria,[a] Hiromu Kaneyoshi,[b] Krzysztof Matyjaszewski,*[b] and Rinaldo Poli*[a]

Abstract: The molecular structure of bis(acetylacetonate)cobalt(II) ([Co(acac)$_2$]) in solution and in the presence of the electron donors (ED) pyridine (py), NEt_3, and vinyl acetate (VOAc) was investigated using ^{1}H NMR spectroscopy in C_6D_6. The extent of formation of ligand adducts, [Co(acac)$_2$(ED)$_x$], varies in the order py > NEt_3 > VOAc (no interaction). Density functional theory (DFT) calculations on a model system agree with Co–ED bond strengths decreasing in the same order. The effect of electron donors on the [Co(acac)$_2$]-mediated radical polymerization of VOAc was examined at 30 °C by the addition of excess py or NEt_3 to the complex in the molar ratio [VOAc]$_0$/[Co]$_0$/[V-70]$_0$/[py or NEt_3]$_0$ = 500:1:1:30 (V-70 = 2,2′-azobis(4-methoxy-2,4-dimethylvaleronitrile)). As previously reported by R. Jerome et al., the polymerization showed long induction periods in the absence of ED. However, a controlled polymerization without an induction period took place in the presence of ED, though the level of control was poorer. The effective polymerization rate decreased in the order py > NEt_3. A similar behavior was found when these electron donors were added to an ongoing [Co(acac)$_2$]-mediated radical polymerization of VOAc. On the basis of the NMR and DFT studies, it is proposed that the polymerization is controlled by the reversible homolytic cleavage of an organocobalt(III) dormant species in the presence of ED. Conversely, the faster polymerization after the induction period in the absence of ED is due to a degenerative transfer process with the radicals produced by the continuous decomposition of the excess initiator. Complementary experiments provide additional results in agreement with this interpretation.

Keywords: bond cleavage · cobalt · degenerative transfer · density functional calculations · radical polymerization

Introduction

Recent progress in controlled radical polymerization (CRP)[1,2] processes allows the synthesis of various well-defined polymer structures in a controlled fashion. Three different CRP mechanisms have been extensively investigated (Scheme 1).[3] The first mechanism (Scheme 1a) is based on a spontaneous reversible homolytic cleavage of a dormant

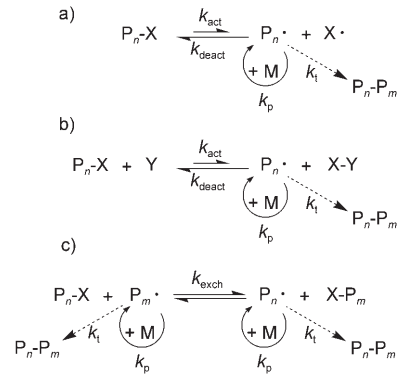

Scheme 1. General mechanisms for three controlled/"living" radical polymerizations (a–c).

[a] S. Maria, Prof. R. Poli
Laboratoire de Chimie de Coordination
UPR CNRS 8241 liée par convention à l'Université Paul Sabatier
et à l'Institut National Polytechnique de Toulouse
205 Route de Narbonne, 31077 Toulouse Cedex (France)
E-mail: poli@lcc-toulouse.fr

[b] H. Kaneyoshi, Prof. K. Matyjaszewski
Center for Macromolecular Engineering, Department of Chemistry,
Carnegie Mellon University
4400 Fifth Avenue, Pittsburgh, Pennsylvania 15213 (USA)

Supporting information for this article is available on the WWW under http://www.chemeurj.org/ or from the author.

chain end and is exemplified by nitroxide-mediated polymerization (NMP)[4] or organometallic radical polymerization (OMRP).[5–14] The second process (Scheme 1b) involves a catalytic reversible homolytic cleavage of a carbon–halogen bond through a redox process, which occurs in atom-transfer radical polymerization (ATRP).[15–19] The third one (Scheme 1c) is based on a thermodynamically neutral bimolecular exchange between propagating radicals and a dormant species. Degenerative transfer (DT) polymerization with alkyl iodides,[20,21] organotellurium, or organostibine species[22] belongs in this category, as well as reversible addition-fragmentation chain-transfer (RAFT)[23] polymerization and macromolecular architecture design by interchange of xanthates (MADIX).[24] Recently, organocobalt compounds have been shown to provide the controlled polymerization of acrylates, acrylic acid, and vinyl acetate by this degenerative transfer mechanism.[25,26]

One of the most promising CRP processes for conducting a successful controlled polymerization of VOAc is the recently reported [Co(acac)$_2$]-mediated polymerization.[9,10] This was initiated with 2,2′-azobis(4-methoxy-2,4-dimethylvaleronitrile) (V-70) in the presence of bis(acetylacetonate)-cobalt(II) ([Co(acac)$_2$]), resulting in the formation of poly(vinyl acetate) (PVOAc) with predetermined M_n and low polydispersity. This system has been proposed to follow the OMRP mechanism in Scheme 1a, with X = Co(acac)$_2$). There is, however, an important feature of this efficient polymerization system that needs clarification. It concerns the puzzling long induction times when the polymerization is carried out in bulk. The offered explanation[9] was based on the effect of the unreacted [Co(acac)$_2$] on the radical dissociation equilibrium (a manifestation of the persistent radical effect). In other words, the radical dissociation equilibrium would lie far to the side of the organocobalt(III) species until nearly all the [Co(acac)$_2$] complex was consumed, followed by the establishment of an equilibrium that is suitably placed to ensure a rapid and controlled polymerization process. However, it is hard to accept that a persistent radical effect could result in such a sharp transition for the free radical concentration. We herein propose an alternative explanation to account for all the observed data.

The second feature is related to the exact nature of the [Co(acac)$_2$] species in solution under the polymerization conditions. The nature of [Co(acac)$_2$] in noncoordinating solvents has been addressed by Cotton and Soderberg on the basis of visible and near-IR spectroscopy. The compound is mononuclear tetrahedral in dilute solutions, whereas it affords octahedral coordination through the formation of oligonuclear aggregates at higher concentrations.[27] An early X-ray diffraction study of anhydrous [Co(acac)$_2$], obtained by sublimation, showed a tetranuclear [Co$_4$(acac)$_8$] arrangement, in which octahedral coordination for the Co^{II} ions is achieved by the sharing of oxygen donors.[28] A different polymorph, described as containing square-planar mononuclear units, has been characterized more recently.[29] The authors underline the absence of significant intermolecular interactions, but a closer look at the molecular packing (structure retrieved from the Cambridge Crystallographic Data Centre)[29] reveals that the molecules are in fact loosely stacked on top of each other as shown in Scheme 2a. Thus,

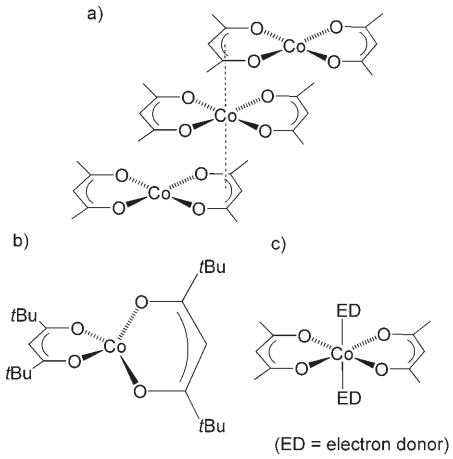

Scheme 2. Schematic representations of the molecular structures found for [Co(acac)$_2$][29], [Co{*t*BuC(O)CHC(O)*t*Bu}$_2$],[30,31] and [Co(acac)$_2$(ED)$_2$].

each Co atom is effectively 6-coordinated, with the fifth and sixth axial coordination positions being occupied by the π-delocalized electron density of the acac ligand of neighboring molecules. A sterically more encumbered analogue, [Co{*t*BuC(O)CHC(O)*t*Bu}$_2$], on the other hand, adopts a tetrahedral structure rather than a square-planar arrangement, as shown in Scheme 2b.[30,31] It is also known that the addition of small amounts of neutral donors yields complex equilibria. For instance, the addition of pyridine yields complexes having py:Co ratios of 1:2, 1:1, and 2:1, the first two species being described as dinuclear, [{Co(acac)$_2$}$_2$(py)] and [{Co(acac)$_2$(py)}$_2$].[32] Indeed, X-ray crystallography shows that the analogous 1:1 adduct with water is dinuclear, [{Co(acac)$_2$(H$_2$O)}$_2$],[33] but a mononuclear five-coordinate [Co(acac)$_2$(ED)] adduct (ED = electron donor) has also been crystallographically characterized for ED = 2-aminopyridine.[34] Many EDs have been shown to add to [Co(acac)$_2$] and yield 1:2 adducts, [Co(acac)$_2$(ED)$_2$]. X-ray crystallographic analyses of numerous derivatives (e.g. ED = H$_2$O,[33,35] MeOH,[36] pyridine,[37] or imidazole,[38]), revealed that these complexes have a *trans*-octahedral geometry, as shown in Scheme 2c. All these observations indicate the propensity of [Co(acac)$_2$] to establish weak coordinative interactions with electron donors leading to octahedral coordination. It is reasonable to ask, therefore, whether the monomer vinyl acetate might be able to establish a coordinative interaction with [Co(acac)$_2$] through the oxygen lone pairs of the ester function, since the bulk CRP of VOAc mediated by [Co(acac)$_2$] with V-70 is conducted in the presence of excess VOAc compared to [Co(acac)$_2$] ([VOAc]$_0$/[Co]$_0$ > 100) at 30 °C.[9–12]

Moreover, the cobalt complex proposed as the dormant species in Scheme 1a (X = Co(acac)$_2$) is only pentacoordi-

nate, whereas Co^{III} is known to strongly prefer a six-coordinate, octahedral geometry. This suggests that one molecule of reactant or other available ED may occupy the sixth available coordination site. In this report, we explore the molecular structure of the [$Co(acac)_2$] complex in solution using ^{1}H NMR spectroscopy and DFT calculations. The effect of EDs such as py and triethylamine on the [$Co(acac)_2$]-mediated polymerization of VOAc is also discussed. This work has allowed correlation of the catalytic performance of [$Co(acac)_2$] with the nature of the EDs and to reveal a previously unsuspected interplay, which is tuned by the ED coordination, between OMRP and DT pathways.

Experimental Section

Characterization: ^{1}H NMR spectra were collected at 30 °C by using a Bruker 250 MHz spectrometer. Deuterated benzene and [D_6]acetone were degassed and stocked in a Schlenk tube on molecular sieves, under argon. The vinyl acetate (VOAc) conversion was either determined by gas chromatography (GC) using a Shimadzu GC 14 A gas chromatograph equipped with an FID detector and a ValcoBond 30 m VB WAX Megabore column, or calculated by the mass ratio before and after the complete removal of residual monomer by evaporation until achievement of constant weight. Toluene or *p*-dimethoxybenzene was used as an internal standard for GC. The molecular weight and molecular-weight distribution of the PVOAc were measured by gel-permeation chromatography (GPC) with PSS columns (styrogel 10^5, 10^3, 10^2 Å) and RI detector (molecular weights and polydispersity indices of the PVOAc were determined relative to linear poly(methyl methacrylate) calibration standards using toluene as an internal standard) or with a 300×7.5 mm PLgel 5 m Mixed-D column (Polymer Laboratories), equipped with multi-angle light scattering (miniDawn Tristar, Wyatt Technology Corp.) and refractive index (RI2000, Soparès) detectors. GPC for the PVOAc was performed using THF as eluent at a flow rate of 1 mL min^{-1} at 35 °C.

Materials: Dinitrogen was purified by passing through a column of anhydrous calcium sulfate. Vinyl acetate (Aldrich, >99%) was passed through a neutral alumina column to remove the stabilizer, dried over calcium hydride, distilled under reduced pressure, and degassed with dinitrogen. Pyridine (Fisher Scientific, 99.9%) and triethylamine (NEt_3, Aldrich, 99.5%) were dried over calcium hydride and degassed with dinitrogen or argon. Toluene (Fisher Scientific, >99%) was distilled over sodium/benzophenone and degassed with dinitrogen. Acetone (sds, >99%) was distilled over calcium sulfate and degassed with argon. Heptane (sds, >99.5%) was distilled over calcium hydride and degassed with argon. Bis(acetylacetonate)cobalt(II) ([$Co(acac)_2$]; Acros, 99%), 2,2′-azobis(4-methoxy-2,4-dimethylvaleronitrile) (V-70; Wako, 96%), *p*-dimethoxybenzene (Aldrich, 99%), and deuterated benzene (Cambridge Isotope Lab, >99.5% D) were used as received.

Initial addition of electron donors to the [$Co(acac)_2$]-mediated VOAc polymerization with V-70: Generally, the polymerizations were conducted by using standard Schlenk techniques. The monomer was deoxygenated by dinitrogen bubbling for 30 min prior to addition to the reaction flask. *p*-Dimethoxybenzene (internal standard for GC, 100 mg), [$Co(acac)_2$] (28.0 mg, 1.09×10^{-4} mol), and V-70 (33.5 mg, 1.09×10^{-4} mol) were placed in a Schlenk flask (25 mL) equipped with a magnetic stirring bar at room temperature. This flask was evacuated in vacuum with cooling in a liquid nitrogen bath and backfilled with dinitrogen. This process was repeated three times with cooling. VOAc (5.0 mL, 5.43×10^{-2} mol) and pyridine (0.26 mL, 3.21×10^{-3} mol) were added to this flask, and the resulting mixture was stirred at room temperature, forming an orange solution. After taking an initial sample for GC, the polymerization was initiated by heating at 30 °C. Aliquots were withdrawn periodically by a syringe to follow the kinetics of the polymerization process. After 45 h, the stirring bar stopped spinning due to the high viscosity of the polymerization medium. The lap samples were diluted with acetone prior to analysis by GC. After the GC measurement, the solvent was changed to THF for GPC. The polymerization in the presence of triethylamine was carried out by an identical procedure, except that NEt_3 (0.45 mL, 3.23×10^{-3} mol) was added instead of pyridine, and deoxygenated toluene (0.2 mL) was used as an internal standard for GC.

Addition of electron donors to the ongoing [$Co(acac)_2$]-mediated VOAc polymerization with V-70: The basic procedure was similar to that described in the preceding section. [$Co(acac)_2$] (55.8 mg, 2.17×10^{-4} mol) and V-70 (66.9 mg, 2.17×10^{-4} mol) were placed in a Schlenk flask (25 mL) equipped with a magnetic stirring bar at room temperature. This flask was evacuated under vacuum with cooling in a liquid nitrogen bath and backfilled with nitrogen. This process was repeated three times with cooling. VOAc (10.0 mL, 1.09×10^{-1} mol) and toluene (0.5 mL) were added to this flask, and the resulting mixture was stirred at room temperature (purple suspension). After taking an initial sample for GC, the mixture was heated at 30 °C to initiate the polymerization. Aliquots were withdrawn periodically using a syringe to follow the kinetics of the polymerization process. After 38 h, two 2.5 mL aliquots of the reaction mixture ([$Co(acac)_2$], 5.42×10^{-5} mol) were placed into separate deoxygenated Schlenk flasks at room temperature The appropriate amount of electron donor (pyridine (0.13 mL, 1.61×10^{-3} mol) or NEt_3 (0.23 mL, 1.65×10^{-3} mol)) was then injected using a syringe. These two flasks and the initial flask were reheated at 30 °C in the same oil bath in order to continue the polymerization. The lap samples were diluted with acetone prior to analysis by GC. After the GC measurement, the solvent was changed to THF for GPC.

[$Co(acac)_2$]-mediated VOAc polymerization with PVOAc macroinitiator:

Synthesis of PVOAC end-capped by cobalt complex: [$Co(acac)_2$] (26 mg, 1.01×10^{-4} mol) and V-70 (186.8 mg, 6.06×10^{-4} mol) were placed in a Schlenk flask equipped with a magnetic stirring bar at room temperature. This flask was evacuated under vacuum with cooling in a liquid nitrogen bath and backfilled with argon. This process was repeated three times with cooling. VOAc (4.0 mL, 4.34×10^{-2} mol) was added to this flask, and the mixture was heated to 30 °C to start the polymerization. After 16 h (43% conversion), the polymerization was quenched and VOAc was evaporated under vacuum. The polymer was then dissolved in acetone, (re)precipitated with heptane, filtered, and dried under reduced pressure. The isolated PVOAc was obtained as a pink solid (M_n=8446; PDI=1.14). The color of the isolated PVOAc was green when wet acetone was used.

Chain extension: The PVOAc end-capped with cobalt, prepared as described above (441 mg, 5.2×10^{-5} mol), was placed in a Schlenk flask equipped with a magnetic stirring bar at room temperature. This flask was evacuated under vacuum with cooling in a liquid nitrogen bath and backfilled with argon. This process was repeated three times with cooling. VOAc (6.0 mL, 6.50×10^{-2} mol) was added to this flask, and the mixture was heated to 30 °C to initiate the polymerization. Aliquots were withdrawn periodically using a syringe to follow the kinetics of the polymerization process.

Computational details: All geometry optimizations were performed using the B3LYP three-parameter hybrid density functional method of Becke,[39] as implemented in the Gaussian 03 suite of programs.[40] The basis functions consisted of the standard 6–31G** for all light atoms (H, C, O), plus the LANL2DZ function, which included the Hay and Wadt effective core potentials (ECP),[41] for Co. The latter basis set was, however, augmented with an *f* polarization function (α=0.8) in order to obtain a balanced basis set and to improve the angular flexibility of the metal functions. All geometry optimizations were carried out without any symmetry constraint and all final geometries were characterized as local minima of the potential energy surface (PES) by verifying that all second derivatives of the energy were positive. The unrestricted formulation was used for open-shell molecules. The mean value of the spin of the first-order electron wave function, which is not an exact eigenstate of S^2 for unrestricted calculations on open-shell systems, was considered to identify the spin state unambiguously. The value of $\langle S^2\rangle$ at convergence was very close to the expected value of 0.75 for doublets, 2 for triplets, and 3.75 for quartets, indicating minor spin contamination.

Results

^{1}H NMR investigation of [Co(acac)$_2$] in the presence of EDs: As discussed in the introduction, [Co(acac)$_2$] is known to be capable of adding electron-donor (ED) molecules, establishing sometimes complex equilibria depending on the nature of the ED and the amount of added ED. We wished to learn more about the interaction between [Co(acac)$_2$] and specific ED molecules under polymerization conditions by using spectroscopic tools. Co^{II} coordination compounds are paramagnetic and could in principle be investigated by EPR spectroscopy. However, the rapid spin relaxation associated with the quartet state does not allow the detection of a spectrum at room temperature or above. To the best of our knowledge, no EPR studies of [Co(acac)$_2$(ED)$_2$] complexes have been reported, and solutions of [Co(acac)$_2$] itself in toluene are described as EPR-silent.[42] We therefore turned to NMR investigations. Indeed, the rapid relaxation of the electron-spin magnetization (conditions leading to very broad EPR resonances) favor the observation of relatively sharp (though paramagnetically shifted) NMR resonances.[43,44] To the best of our knowledge, NMR investigations of Co^{II} acetylacetonate complexes are unprecedented.

Dissolution of anhydrous [Co(acac)$_2$] in C_6D_6 yields a homogeneous purple solution which shows only one very broad resonance centered at around -1 ppm ($w_{1/2}=860$ Hz), see Figure 1a. We attribute this resonance to the twelve equivalent CH_3 protons of the acac ligand. The signal corresponding to the CH protons could not be identified. We presume that it is either overshadowed by the broad CH_3 resonance, or broadened beyond detection and lost in the baseline. Indeed, the metal spin density is probably transmitted more efficiently onto the acac CH proton, because it is directly linked to the conjugated Co–acac system. The addition of VOAc to this solution yields no significant color change and the resulting ^{1}H NMR spectrum is the superposition of the broad [Co(acac)$_2$] resonance (with essentially unchanged linewidth and chemical shift) and the sharp resonances of free VOAc. The amount of added VOAc affects only the relative intensity of the free VOAc resonances, while it does not significantly affect their chemical shift and linewidth. This observation implies the absence of a significant [Co(acac)$_2$]–VOAc interaction.

The addition of py to the [Co(acac)$_2$] solution results in an immediate color change from purple to orange, indicating the formation of [Co(acac)$_2$(py)$_x$] adducts. The color of the *trans*-[Co(acac)$_2$(py)$_2$] complex has been reported to be orange.[37] The color change was accompanied by dramatic changes in the NMR spectrum, as seen in Figure 1b–d. The free ligand resonance is already visible after the addition of approximatelly one equivalent. On the other hand, the [Co(acac)$_2$] resonance disappears immediately after the first py addition and is replaced by new resonances for the py adduct(s). This is consistent with the solution equilibria that have previously been established by the spectrophotometric study,[32] as summarized in Scheme 3. According to that study, the first addition, leading to [{Co(acac)$_2$}$_2$(py)], is essentially quantitative, whereas the equilibrium constant K_2 is only around 2.0. Thus, a significant amount of free py would remain present after the addition of one equivalent, together with a mixture of [{Co(acac)$_2$}$_2$(py)], [Co(acac)$_2$(py)], and [Co(acac)$_2$(py)$_2$]. The resonances of the paramagnetic complexes, as well as that of free py, shift as a function of the added py amount. This indicates that an exchange occurs between the free and coordinated py molecules, and that this is in the slow-exchange limit. Note, however, that only one set of resonances is observable for the cobalt complexes. Each resonance of this set becomes sharper and its chemical shift is convergent upon addition of a larger py excess, in which the [Co(acac)$_2$(py)$_2$] species is predominant. For each proton, the chemical shift difference ($\Delta\nu$) between different [Co(acac)$_2$(py)$_x$] complexes is likely to be greater than the $\Delta\nu$ between free and coordinated pyridine. Therefore, the failure to observe individual sets of resonances for the individual cobalt complexes cannot be attributed to fast exchange. It is more likely that the resonances of complexes [{Co(acac)$_2$}$_2$(py)] and [Co(acac)$_2$(py)] are not detected because they are broader, less intense (especially at the higher

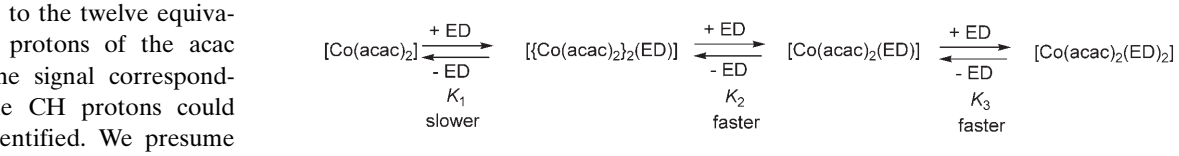

Scheme 3. Mechanism of ligand (ED) addition and exchange on [Co(acac)$_2$].

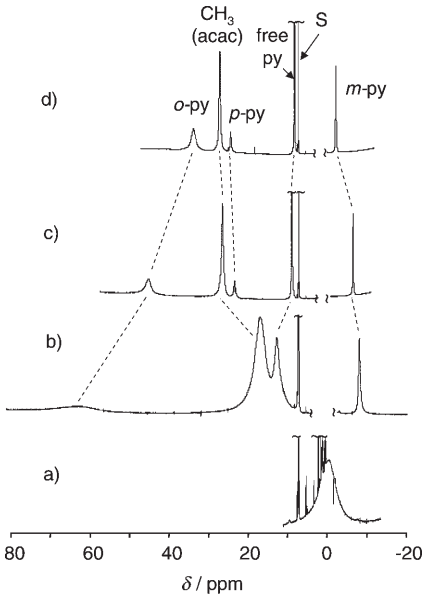

Figure 1. ^{1}H NMR spectra in C_6D_6 of the mixture of [Co(acac)$_2$] with py: a) no added ligand; b) 1 equiv; c) 2 equiv; d) 3 equiv.

py/Co ratios), and more paramagnetically shifted. The last proposition is proven by the direction in which each resonance shifts as a function of the py/Co ratio. Inspection of the relative integrated intensities, paramagnetic shifts, and line widths leads to the resonance assignment given in Figure 1. It is interesting to note how the acac resonance continuously shifts and sharpens from the value of free [Co(acac)$_2$] to that of [Co(acac)$_2$(py)$_2$]. This behavior suggests that the observed resonance for pure [Co(acac)$_2$] results from the rapid equilibration between mononuclear and oligonuclear species. The small resonance of the *p*-py proton is not visible in the py/Co = 1 spectrum, because it is overshadowed by the stronger acac and free py resonances.

Contrary to the effect of pyridine and similarly to the effect of VOAc, the addition of NEt_3 to the [Co(acac)$_2$] solution results in no significant color change. The NMR behavior, however, is different from both. After the addition of one equivalent, new broad peaks of relatively small intensity that can be attributed to free NEt_3 become visible, as indicated by the black arrows in Figure 2a, while a broad resonance is still present in the region of free [Co(acac)$_2$] (white arrow). The free NEt_3 resonances, especially the one attributed to the CH_2 group, exhibit a paramagnetic shift ($\delta =$ 7.86 ppm for CH_2, 0.94 ppm for CH_3; compare with 2.50 and 1.06 ppm in the absence of the Co complex). Further addition of a second NEt_3 equivalent affords a very large increase of the free NEt_3 resonances and a shift to $\delta = 7.56$ (CH_2) and 0.97 (CH_3), while the broad [Co(acac)$_2$] resonance is still present, Figure 2b. A fourfold increase in the amount of NEt_3 produces a further resonance shift to $\delta =$ 6.66 and 1.01 ppm, while the free [Co(acac)$_2$] resonance has now essentially disappeared, as shown in Figure 2c. Continued NEt_3 addition further shifts the free Et_3N resonances toward the diamagnetic position (e.g. $\delta \approx 3.0$ ppm for the CH_3 protons after the addition of 30 equivalents). The resonances of the coordinated NEt_3 and acac ligands in [Co(acac)$_2$(NEt$_3$)$_x$] complexes are not visible. At the same time, the resonance of free [Co(acac)$_2$] remains unshifted and unbroadened. These results can be rationalized on the basis of the same scheme invoked for the py system (Scheme 3).[32] The observations prove that NEt_3, like py, forms adducts with [Co(acac)$_2$], but the equilibria are far less in favor of the addition products (that is, K_1, K_2 and K_3 are smaller). As for the py system, an exchange occurs between free and coordinated NEt_3 molecules. A bis adduct forms to a much lower extent or not at all, or its resonances are much broader because of a faster ligand-exchange process. The observation of the unshifted [Co(acac)$_2$] resonance at low NEt_3/Co ratios shows that this complex is not involved in the amine exchange process. This means that the NEt_3 exchange probably involves the different NEt_3 adducts, rather than dissociation to yield the [Co(acac)$_2$] starting compound.

Since water is a possible contaminant of [Co(acac)$_2$] and since the VOAc polymerization was also successfully carried out under suspension and miniemulsion conditions,[10,13] additional NMR experiments were carried out by deliberately adding water. The addition of water to a solution of [Co(acac)$_2$] in C_6D_6 caused the immediate precipitation of a pale solid, presumably [Co(acac)$_2$(H$_2$O)$_2$], which is described as sparingly soluble in nonpolar organic solvents.[33,35] In order to avoid the precipitation process, subsequent analyses were carried out in [D$_6$]acetone.

First, the spectrum of [Co(acac)$_2$] in [D$_6$]acetone was recorded before the addition of water, see Figure 3a. This shows two broad ($w_{1/2} \approx 400$ Hz) resonances at $\delta \approx 6.8$ and 9.4 ppm that can be assigned either to the CH_3 and CH resonances of the acac ligand in a single compound, or to the CH_3 resonances of two different compounds. The latter possibility appears more likely since the CH resonance has not been observed for any of the other spectra (see also below). The nature of the second compound, however, is unclear. The shift and sharpening of the [Co(acac)$_2$] resonance from the value observed in C_6D_6 suggests that an interaction with the acetone solvent has taken place. It is interesting to compare this result with the lack of any interaction between [Co(acac)$_2$] and VOAc. Evidently, the replacement of the

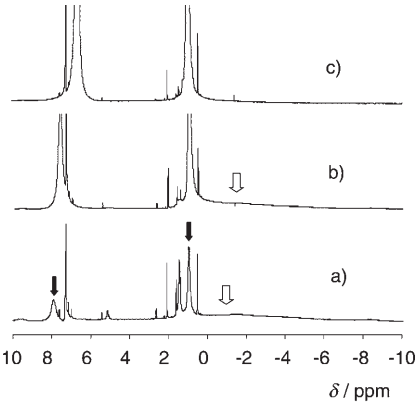

Figure 2. ^{1}H NMR spectra in C_6D_6 of the mixture of [Co(acac)$_2$] with NEt_3: a) 1 equiv; b) 2 equiv; c) 4 equiv.

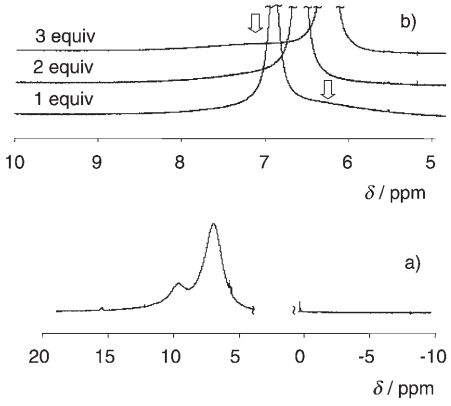

Figure 3. ^{1}H NMR spectra of [Co(acac)$_2$]/NEt_3 mixtures in [D$_6$]acetone: a) before NEt_3 addition; b) after the addition of 1–3 equivalents.

alkoxo group in VOAc by a methyl group in acetone significantly improves the donor properties of the carbonyl function. The subsequent addition of small amounts of water to this solution caused precipitation, indicating that the acetone ligands were replaced by water molecules. It is also interesting to analyze the spectral changes observed upon addition of NEt_3 in [D_6]acetone, see Figure 3b, and to compare them with those observed in C_6D_6. The broad resonance centered around $\delta = 6.8$ ppm remains visible, even after the addition of three equivalents of NEt_3, and does not shift significantly with the amount of excess NEt_3. At the same time, the free NEt_3 resonance is paramagnetically shifted to a lesser extent relative to the corresponding experiment in C_6D_6 ($\delta = 6$–7 ppm in [D_6]acetone, compared to $\delta = 8$–7 ppm in C_6D_6). This is in agreement with the expected smaller extent of NEt_3 coordination to [Co(acac)$_2$], since the acetone solvent is now competing for the coordination sites on Co^{II}. The broad resonance observed for the [Co(acac)$_2$] around $\delta = 9.4$ ppm (Figure 3a), on the other hand, is no longer visible. The addition, to this solution, of small amounts of water, again led to the formation of a pale precipitate. However, subsequent addition of pyridine caused the redissolution of this precipitate and the formation of an orange solution, the ^{1}H NMR spectrum of which is identical to that shown in Figure 1.

In conclusion, these NMR experiments indicate a relative affinity of various ED molecules for coordination to [Co(acac)$_2$] in the order VOAc (no coordination) < NEt_3 < acetone < H_2O < pyridine. They also indicate the presence of an exchange between free and coordinated ED molecules, the rate of exchange being faster for the less strongly coordinated ligands. In the presence of excess ED, the cobalt center undergoes less ligand dissociation and exchange, as evident from the relatively sharp paramagnetically shifted resonances in the case of pyridine. For the less tightly bound ligands, the NMR spectrum is not visible and no structural information is furnished by the experiment, but equilibria between lower coordinate species, mono- and/or dinuclear, are probably occurring rapidly.

Computational investigation of the [Co(acac)$_2$] structure and interactions with EDs: The adoption of a tetrahedral structure for [Co{*t*BuC(O)CHC(O)*t*Bu}$_2$][30,31] suggests an electronic preference for a tetrahedral environment around four-coordinate Co^{II}, whereas a *trans*-octahedral geometry is adopted in the presence of EDs. However, the steric demand of the *t*Bu substituents may be responsible for this choice. Previous spectrophotometric studies have provided evidence that [Co(acac)$_2$] is a tetrahedral monomer, like its *t*Bu analogue, in dilute solution.[27] We used DFT calculations to further confirm this conclusion. [Co(acac)$_2$] was optimized in both the tetrahedral and the square-planar geometry. In the former case, only the high spin ($S = 3/2$) configuration was considered, since no low-spin tetrahedral complex for any d^4–d^7 metal is know with low-field ligands.[45] The square-planar geometry, on the other hand, generates a high-energy $d_{x^2-y^2}$ orbital, possibly resulting in spin pairing, thus both doublet and quartet spin states were considered. The results of the calculations are listed in Table 1. In agreement with the experimental study, the lowest energy is found for the quartet tetrahedral geometry. Although no symmetry was imposed in the calculation, the geometry converged to an essentially perfect D_{2d} symmetry. The optimized Co–O distance (1.945 Å) and O–Co–O angle (95.8°) are quite close to those determined experimentally for [Co{(*t*BuCO)$_2$CH}$_2$] (1.934 Å and 95.4°, respectively).[31] The square-planar geometry gave a stable minimum only in the doublet state, a few kcal mol^{-1} higher than the lower tetrahedral quartet. Attempts to optimize a quartet square-planar geometry led to the rearrangement to the tetrahedral minimum.

Table 1.
DFT-optimized energies [in kcal mol^{-1}] of [Co(acac)$_2$(ED)$_n$] ($n = 0$, 1, 2), relative to [Co(acac)$_2$ + n(ED)].

n	ED	Geometry[a]	S	E
0	–	tet	3/2	0
	–	sp	1/2	8.80
1	CH_3COOCH_3	tbp	3/2	−0.91
	$N(CH_3)_3$	tbp	3/2	−5.26
	py	tbp	3/2	−5.77
	H_2O	tbp	3/2	−7.38
	H_2O	spy	3/2	−3.77
	NH_3	tbp	3/2	−10.17
2	CH_3COOCH_3	oct	3/2	−5.40
	$N(CH_3)_3$	oct	3/2	−10.89
	py	oct	3/2	−11.40
	H_2O	oct	3/2	−18.85
	NH_3	oct	3/2	−23.84

[a] tet = tetrahedral; sp = square planar; tbp = trigonal bipyramidal; spy = square pyramidal; oct = octahedral.

The main thrust of our computational investigation concerns the equilibria affecting the radical concentration under polymerization conditions, and how these are modified by the introduction of electron donors. We therefore studied the binding of ED molecules to the [Co(acac)$_2$] catalyst and to the [R–Co(acac)$_2$] dormant species. However, we limited our investigation to mononuclear complexes. The Co^{III} system is most likely to be present in the six-coordinate [R–Co(acac)$_2$(ED)] form. Ligand dissociation to give mononuclear [R–Co(acac)$_2$] was considered, but the possible dimerization of the latter was not. The activation process generates the mononuclear [Co(acac)$_2$(ED)] or [Co(acac)$_2$] complexes, which may yield dinuclear or oligonuclear aggregates. We limited our study to the equilibria of the above two mononuclear Co^{II} complexes with each other and with the octahedral complex [Co(acac)$_2$(ED)$_2$]. The results of these investigations can address, at least qualitatively, the nature of the polymerization process under conditions of excess ED. An additional cautionary note concerns the neglect of entropy contributions. A statistical mechanics analysis of the entropic term by using the partition function is only possible in the gas phase, whereas the polymerization

reactions are carried out in condensed phases. Therefore, the conclusions drawn can only be qualitatively based on the bond energy values.

Compound CH_3COOCH_3 was selected as a model for VOAc. Since bonding is established by the carbonyl O atom, which is not conjugated with the vinyl function, this replacement is not expected to change the donor properties of the ester function and reduces the computational effort. Pyridine was used as such, whereas NEt_3 was modeled with NMe_3 and NH_3, allowing a partial probing of steric effects. Finally, H_2O was also used as an ED. Concerning the Co^{III} dormant species, CH_3 was chosen as a model for the R group. Although the resulting R–Co bond dissociation energies (BDEs) will be unrealistic, the trends obtained for the different ED molecules should be qualitatively relevant.

The addition of a single ED molecule affords [Co(acac)$_2$(ED)] structures with a trigonal bipyramidal geometry, as shown in Table 1. The possibility of the alternative square planar geometry was explored with ED = H_2O, but resulted in a higher energy. All investigated molecules converged to similar trigonal-bipyramidal structures in the quartet state. The interaction energy increases in the order $CH_3COOCH_3 < N(CH_3)_3 \sim py < NH_3 < H_2O$. It is interesting to note the very weak interaction with the carbonyl function of CH_3COOCH_3, whereas NMe_3 and py form Co–N bonds of approximately equal strength. The Co–OH_2 and Co–NH_3 bonds are stronger still. The last two systems exhibit a significant distortion, with one close contact between one of the ED protons and one of the axial acac O atoms (O–H···O = 1.894 Å for ED = H_2O, N–H···O = 2.232 Å for ED = NH_3) suggesting the presence of a hydrogen-bonding interaction. In agreement with this hypothesis, the bond angles between the Co–O(N) and O(N)–H bonds are correspondingly smaller than expected (Co-O-H = 91.7° compared to 113.5° for the other O–H bond; Co-N–H = 101.8° compared to 114.0° and 114.2° for the other N–H bonds). This phenomenon may be partially responsible for the additional stability of these adducts relative to the other ED's which lack active protons. However, we must also consider that the stabilization energy is calculated relative to isolated [Co(acac)$_2$] and H_2O or NH_3 molecules in the gas phase. In condensed phases (for instance, in toluene) these protic ED molecules form aggregates, therefore reducing the energetic gain of the Co–H_2O or Co–NH_3 bond formation. The difference between NH_3 and NMe_3 could in part be due also to the increased steric demand imposed by the three Me groups. By extrapolation, we can predict that the binding energy of the Co–NEt_3 bond will be smaller relative to the Co–py bond, in agreement with the NMR results.

The above trends remain unchanged upon going to the *trans*-Co(acac)$_2$(ED)$_2$ systems. As shown in Table 1, binding the second ED molecule results in each case in a slightly greater energy gain relative to the first one, consistent with the general tendency of Co(acac)$_2$ to form octahedral complexes rather than five-coordinate ones by the addition of EDs. The optimized coordination geometries are in general quite close to octahedral, with the two acac ligands being approximately coplanar. The H_2O and NH_3 adducts exhibit a distortion that consists of a "flap" of the two acac ligands around the O···O "hinge" axes, in opposite directions. This is particularly evident for the NH_3 derivative, for which the hinge angle (angle between the acac plane and the CoO_2 plane) is 158.85°. The reason for this distortion is not evident, but we note that this is also experimentally observed for the [Co(acac)$_2$(H_2O)$_2$] structure[33] (hinge angle of 162.8° compared to 164.0° for the optimized structure). On going from the NH_3 to the NMe_3 adduct, the two Co–acac six-membered cycles go back to planarity, suggesting that hydrogen-bonding may again be the cause of the distortion. The optimized geometry of the pyridine adduct exhibits the two py ligands orthogonal to each other. This corresponds to the arrangement experimentally observed for *trans*-[Co(acac)$_2$(py)$_2$][37] and for *trans*-[Co(acac)$_2$(4-CH_3py)$_2$].[46] The optimized Co–O and Co–N distances (averages are 2.06 and 2.23 Å) are in good agreement with the experimentally observed ones (2.034(3) and 2.19(1) Å).[37]

The conclusion of this theoretical investigation is that [Co(acac)$_2$] generally forms weak bonds with ED molecules, especially the carbonyl O atom of ester functions. This result is in qualitative agreement with the observation of oxygen-bridged octahedral coordination for tetrameric [Co(acac)$_2$][28] and with the preference of a mononuclear tetrahedral structure for the sterically more encumbered *t*Bu analogue.[30,31] Amines and pyridine bind more strongly, but the steric bulk of NEt_3 should probably reduce the bond formation energy. The calculations overestimate the stability of the H_2O and NH_3 adducts (indeed, the NMR study proves that H_2O binds less strongly than pyridine), because of the incomplete consideration of hydrogen-bonding interactions (neglected for the free ligands).

Computational investigation of the CH_3–Co(acac)$_2$ bond strength and interactions with EDs: The salient results of this study are collected in Table 2. The optimization of five-coordinate CH_3–Co(acac)$_2$ molecule was attempted both as a trigonal bipyramid (tbp) and as a square pyramid (sp). The tbp calculation gave a stable minimum only in the triplet state. Attempts to optimize a tbp geometry in the singlet state led to a rearrangement and convergence of the more stable sp structure. Relative to the separate tetrahedral (S = 3/2) [Co(acac)$_2$] and CH_3 radicals, the singlet sp was more stable by 18.50 kcal mol^{-1}, whereas the triplet tbp was only

Table 2. DFT-optimized energies [in kcal mol^{-1}] of [CH_3–Co(acac)$_2$(ED)$_n$] (n = 0, 1) relative to [Co(acac)$_2$ + CH_3 + n(ED)].

n	ED	Geometry[a]	S	E
0	–	sp	0	−18.50
	–	tbp	1	−6.52
1	CH_3COOCH_3	oct	0	−22.73
	$N(CH_3)_3$	oct	0	−25.91
	py	oct	0	−27.60
	H_2O	oct	0	−30.03
	NH_3	oct	0	−31.97

[a] sp = square planar; tbp = trigonal bipyramidal; oct = octahedral.

stabilized by 6.52 kcal mol^{-1}. The Co^{III} ion is known to be particularly stable in an octahedral coordination environment, thus the presence of ED molecules is expected to lead to dormant species of type [Co(acac)$_2$(PVOAc)(ED)]. The various ED molecules were added to the empty coordination site of the lower energy sp [CH_3–Co(acac)$_2$] molecule to yield *trans*-[Co(acac)$_2$(CH_3)(ED)] adducts. All these molecules were optimized only in the singlet state, as alkylcobalt(III) molecules are known to be diamagnetic.[47] Note, however, that no [R–Co(acac)$_2$] or [R–Co(acac)$_2$(ED)] molecules have been previously described to the best of our knowledge. Axial ED binding to either [CH_3–Co^{III}(acac)$_2$] or to [Co^{II}(acac)$_2$(ED)] results in very similar energetic gains for CH_3COOCH_3 (4.23 vs. 4.49 kcal mol^{-1}), H_2O (11.53 vs. 11.47 kcal mol^{-1}) and NH_3 (13.47 vs. 13.67 kcal mol^{-1}). On the other hand, slightly stronger binding to the alkylcobalt(III) occurs for NMe_3 (7.41 vs. 5.63 kcal mol^{-1}) and especially for py (9.10 vs. 5.63 kcal mol^{-1}).

The stereoelectronic properties of ED could affect the homolytic bond strength of the Co^{III}–C bond (that is, the energy difference between [Co(acac)$_2$(CH_3)(ED)] and the separate {Co(acac)$_2$(ED)} and CH_3 fragments), as previously demonstrated in the chemistry of vitamin B_{12}.[48,49] However, the axial ED nature only has a slight effect on the Co^{III}–CH_3 BDE for this system: 21.82, 20.65, 21.83, 22.65, and 21.80 kcal mol^{-1} for CH_3COOCH_3, NMe_3, py, H_2O, and NH_3, respectively. All these values are greater than the Co^{III}–CH_3 BDE of unsolvated [Co(acac)$_2$(CH_3)] (18.50 kcal mol^{-1}).

It is interesting to compare two processes of relevance to the radical polymerization controlled by [Co(acac)$_2$]: on the one side, the homolytic CH_3–Co bond rupture in the octahedral complex [CH_3–Co(acac)$_2$(ED)]; on the other side, the equilibrium between the resulting five-coordinate [Co(acac)$_2$(ED)] complex and the corresponding bis-adduct, [Co(acac)$_2$(ED)$_2$]. For each ED used in the computational study, the energetics of these two processes are shown on the left and right hand sides of Figure 4, respectively. The absolute values are not useful for evaluating the equilibrium positions and the effective polymerization rates for a variety of reasons, for example, the CH_3 model for the growing polymer chain, and the neglect of entropy. The free energies are in principle less positive for the homolytic bond rupture process and less negative for the ED addition process, relative to the energies shown in Figure 4. However, the figure allows the estimation of qualitative trends. Under the hypothesis of identical entropic contributions for the different ED systems, a greater Co–CH_3 BDE should slow down the effective polymerization rate, whereas a greater stabilization by the ED addition should accelerate the process. The latter phenomenon results from the reduced availability of the [Co(acac)$_2$(ED)] radical trap, and from the fact that the coordinatively saturated [Co(acac)$_2$(ED)$_2$] complex has no trapping ability. Therefore, the kinetic acceleration may also be accompanied by partial or total loss of control.

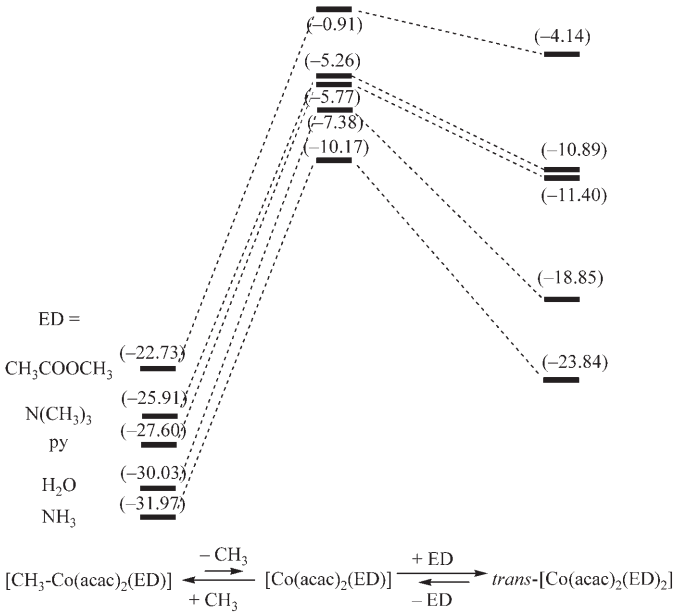

Figure 4. Relative DFT energies for model transformations of relevance to the controlled radical polymerization of VOAc.

Effect of the initial addition of electron donors on the CMRP of VOAc mediated by [Co(acac)$_2$] with V-70: As demonstrated above, N-donor ligands such as py and NEt_3 are able to coordinate to a different extent to [Co(acac)$_2$] (py ≫ NEt_3), producing the [Co(acac)$_2$(ED)$_x$] complex. There is no indication, on the other hand, of the coordination of VOAc to [Co(acac)$_2$]. Therefore, an electron-donating effect originating from the coordinating ED may change the reactivity of a cobalt(II) complex towards a VOAc radical. Accordingly, 30 equivalents of ED (py or NEt_3) compared to cobalt were initially added to the [Co(acac)$_2$]-mediated VOAc polymerization initiated by V-70 at 30 °C ([VOAc]$_0$/[Co(acac)$_2$]$_0$/[V-70]$_0$/[ED]$_0$ = 500:1:1:30). In the absence of ED additives, the reaction medium was initially a purple slurry, then it changed to a brown solution after one day, suggesting the formation of a cobalt(III) species. A rapid polymerization started after an induction period (see the semilogarithmic plot in Figure 5) and the number average molecular weight increased more or less linearly with conversion, with relatively low polydisperties (see Figure 6). The raw data are also reported in tabular form in the Supporting Information. The observed M_n are close to (slightly higher than) those expected for one growing chain per cobalt atom. All these observations are in line with the previous report.[9] Note that our reaction conditions are identical to those used previously, except that we employed a V-70/Co ratio of 1:1 instead of 6.5:1. Consequently, the only major difference in our results with respect to those previously reported is the longer observed induction time (around 30 h).

For the experiment run in the presence of py (30 equivalents), the purple slurry turned immediately to a clear

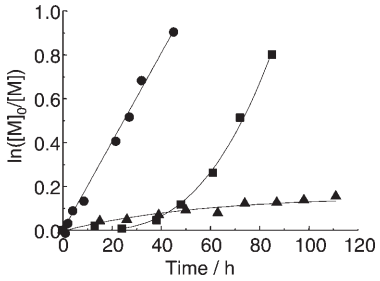

Figure 5. Semilogarithmic kinetic plots for the initial addition of electron donors to bulk CMRP of VOAc mediated by [Co(acac)$_2$] with V-70 at 30 °C ([VOAc]$_0$/[Co(acac)$_2$]$_0$/[V-70]$_0$/[ED]$_0$ = 500:1:1:30): (■) no addition, (●) addition of py (30 equiv), (▲) addition of NEt$_3$ (30 equiv).

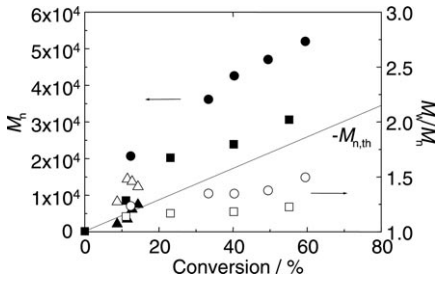

Figure 6. Evolution of M_n and M_w/M_n versus conversion for the initial addition of electron donors to bulk CMRP of VOAc mediated by [Co(acac)$_2$]. Conditions are the same as those given in Figure 5. (■, □) No addition, (●, ○) addition of py (30 equiv), (▲, Δ) addition of NEt$_3$ (30 equiv).

orange solution, as described above. The mixture remained a clear orange solution until the end of the polymerization. While this may suggest the persistence of the Co^{II} species during the polymerization, note that [R–Co(acac)$_2$(ED)] compounds have not previously been described, thus the possibility of formation of an alkylcobalt(III) dormant species that coincidentally had the same color cannot be excluded. In the case of NEt$_3$, the reaction medium quickly turned to a violet slurry, and then it became a mixture of a brown solution and pale purple insoluble materials after one day. The semilogarithmic kinetic plots for the monomer consumption are shown in Figure 5. The first striking observation is that, in the presence of py or NEt$_3$, the polymerizations did not show any induction period. The linearity of the plots suggests that the polymerizations are controlled, which is further confirmed by the evolution of M_n and M_w/M_n versus monomer conversion (see Figure 6). For both polymerizations, M_n increased with conversion and remained close to the theoretical values, while the polydispersity remained in the 1.3–1.5 range and all of the GPC curves displayed a monomodal shape (representative chromatograms are available in the Supporting Information). Although these values are higher than for the PVOAc prepared in the absence of ED, they are typical of CRP processes. The significance of the M_n growth for ED = NEt$_3$ is limited, since the polymerization was very slow and only low conversions (up to 14%) were achieved. However, the isolated polymers had M_n in close agreement with the theoretical values, under the assumption that only one macromolecular chain is generated per cobalt atom. In the case of py, the M_n of PVOAc exhibited a larger departure from the $M_{n,th}$ toward greater values, showing that less than one chain per cobalt is generated. This phenomenon probably results from a combination of slow initiation (the half-life of V-70 is approximately 10 h at 30 °C) and inefficient trapping of the radicals generated by V-70 by the Co^{II}-py system.

Effect of the addition of electron donors to an ongoing CMRP of VOAc mediated by Co(acac)$_2$ with V-70: To further explore the effect of ED coordination to the dormant species on the [Co(acac)$_2$]-mediated VOAc polymerization, excess ED was added to the reaction system after the formation of the dormant species. First, a normal CRP of VOAc was conducted at 30 °C to prepare a dormant species with a PVOAc chain ([VOAc]$_0$/[Co(acac)$_2$]$_0$/[V-70]$_0$ = 500:1:1). After 43 h, the reaction medium (brown solution) was split into three equal parts, and 30 equivalents of py or NEt$_3$ with respect to [Co(acac)$_2$] were injected into two of these mixtures. Subsequently, all three mixtures were reheated at 30 °C in the same bath to continue the polymerization. Figure 7 shows the semilogarithmic kinetic plot, and Figure 8 reports the evolution of M_n and M_w/M_n versus conversion. The data are available in tabular form in the Supporting Information.

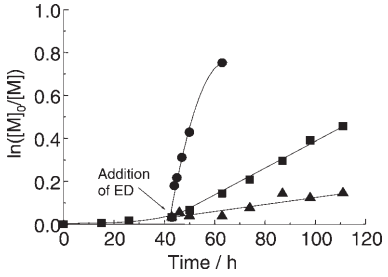

Figure 7. Semilogarithmic kinetic plots for the middle addition of electron donors to bulk CMRP of VOAc mediated by [Co(acac)$_2$]: Conditions are the same as those given in Figure 5. (■) No addition, (●) addition of py (30 equiv), (△) addition of NEt$_3$ (30 equiv).

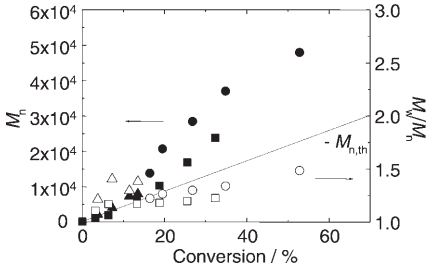

Figure 8. Evolution of M_n and M_w/M_n versus conversion for the later addition of electron donors to bulk CMRP of VOAc mediated by [Co(acac)$_2$]. Conditions are the same as those given in Figure 5.(■, □) No addition, (●, ○) addition of py (30 equiv), (▲, Δ) addition of NEt$_3$ (30 equiv).

Because the half-life of V-70 in toluene at 30 °C is 10 h, almost all the V-70 should already have decomposed after 43 h. Therefore, the predominant compound in the polymerization system will be the $[Co(acac)_2(PVOAc)]$ complex as a dormant species, with the possible additional coordination of a VOAc monomer molecule. After the addition of 30 equivalents of py, the color of the reaction medium immediately changed from a brown solution to a clear orange solution, as was the case for initial addition of py to the reaction medium. Moreover, this mixture became more viscous within one hour, suggesting the production of polymeric materials. In contrast, no color change was observed in the case of the NEt_3 addition. As shown in Figure 7, the semilogarithmic kinetic plot after the addition of excess py displayed the faster rate of polymerization relative to the normal CRP of VOAc. This suggested that the formation of the $[Co(acac)_2(PVOAc)(py)]$ complex led to the release of PVOAc radicals from the dormant species, resulting in an acceleration of the polymerization rate. On the other hand, the rate of polymerization in the presence of excess NEt_3 was slower than that of the normal CRP, despite there being no color change. This implies that the coordination of NEt_3 to the dormant species suppressed the dissociation of the cobalt–PVOAc bond. The evolution of M_n and M_w/M_n versus conversion (Figure 8) is much the same as when the ED molecule was introduced at the beginning, before the formation of the dormant species (Figure 6), and the molecular-weight distribution is once again monomodal (representative chromatograms are available as Supporting Information). These experiments indicate that the addition of the ED molecule changes the nature of the dormant species dramatically, but its effect does not depend upon whether the organocobalt(III) compound is generated in its absence or in its presence.

Interplay of OMRP and DT mechanisms: The controlled growth of PVOAc for the $[Co(acac)_2]$-mediated polymerization in the presence of py or NEt_3, even though the control is not as good as for the polymerization in the absence of ED, strongly suggests that the cobalt complex interacts with the growing chain, establishing an equilibrium with a dormant species. The dramatic difference in polymerization rate as a function of ED (py ≫ NEt_3) confirms that the cobalt complex is directly implicated in this equilibrium. On the basis of the solution NMR investigation and the DFT calculations, it is natural to propose that this control is established via an OMRP equilibrium, namely involving the formation of an organometallic dormant species, as shown in Scheme 4b. The reason for the relative polymerization rate in the order py ≫ NEt_3 can be attributed to the different stabilization of the product of Co^{III}–R bond cleavage, the five-coordinate Co^{II} complex $[Co(acac)_2(ED)]$, upon coordination of a second ED molecule. The NMR investigation indicates that the py addition is more favorable than the NEt_3 addition and the DFT calculations confirm this trend, after consideration of the steric factors from the result of the NMe_3 model system (Figure 4). In addition, the DFT calculations show that the homolytic bond dissociation energy of the Co^{III}–R bond does not change greatly as a function of the ED.

It should be mentioned that, according to the literature,[50] NEt_3 slows down the free radical polymerization of VOAc because of sacrificial H atom transfer from NEt_3 to the growing radical chain. Since the resulting Et_2NCHCH_3 radical is highly stabilized and is not capable of reinitiating the polymerization, this process effectively amounts to a termination event. However, a control experiment carried out under the same conditions as used for the $[Co(acac)_2]$-mediated polymerization (bulk, $[VOAc]_0/[V\text{-}70]_0/[NEt_3]_0 = 500:1:30$, 30 °C) showed that the polymerization rate was only halved relative to the free polymerization in the absence of NEt_3. Therefore the sacrificial H atom transfer from NEt_3 may only account for a small fraction of the dramatic polymerization rate decrease on going from py to NEt_3.

The NMR and DFT studies also indicate that vinyl acetate does not establish a significant interaction with $[Co(acac)_2]$. These results allow us to predict that the spin trap in the absence of ED additive is the simple mononuclear tetrahedral $[Co(acac)_2]$ complex (perhaps in equilibrium with a higher aggregate, according to the literature[27]).

Consequently, the spin trap should not enjoy any particular energetic stabilization in the absence of ED, the equilibrium should be more displaced toward the organocobalt(III) dormant species, and the polymerization should be slower. This indeed corresponds to the experimental evidence from the initial stages of the polymerization process (during the induction period in the absence of ED), but does not account for the fast and controlled polymerization after the initial period.

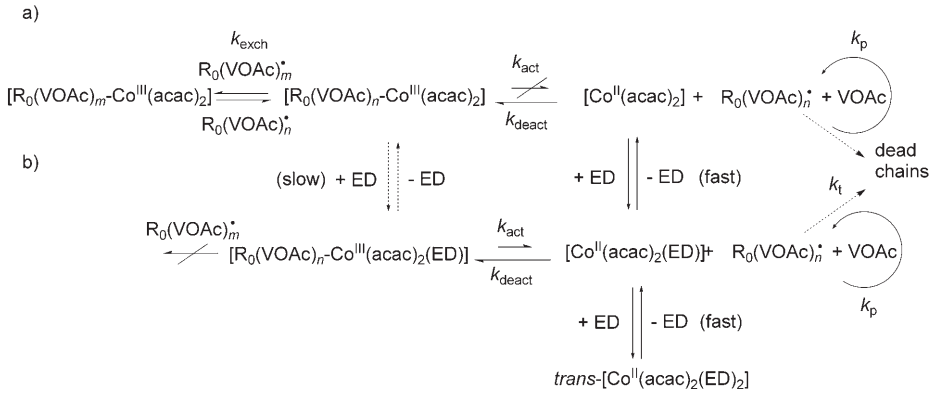

Scheme 4. Proposed general mechanism for the CMRP of VOAc mediated by $[Co(acac)_2]$ complex in the a) absence and b) presence of EDs.

A reasonable explanation for the latter phenomenon must therefore be based on a different mechanism. The radical influx from the V-70 initiator ($t_{1/2}=10$ h at 30 °C) will gradually convert the [Co(acac)$_2$] complex to an organocobalt(III) species in an essentially irreversible process. Towards the end of the transformation of Co^{II} to Co^{III} species, the new radicals will no longer be trapped efficiently and will therefore start to generate polymer chains, explaining the onset of a fast polymerization process. The fact that the polymerization remains controlled can be explained by the intervention of a degenerative transfer (DT) process, as indicated in Scheme 4a. The same control mechanism has been proposed recently for the polymerization of methyl acrylate, acrylic acid, and vinyl acetate by a cobalt–porphyrin system.[25,26] Note that no degenerative transfer mechanism may take place in the presence of ED, because ED blocks the coordination site on the organocobalt(III) dormant species that is necessary for the associative radical exchange. The ED dissociation process from the dormant species (indicated with dashed arrows in Scheme 4) is expected to be slow, because of the well-known inertness of low-spin d^6 coordination compounds. Thus, a DT mechanism may only take place when the ED does not bond strongly with the Co^{III} dormant species, leaving a significant amount of five-coordinate [R_0-(VOAc)$_n$–Co^{III}(acac)$_2$] at equilibrium. Conversely, d^7 complexes are kinetically labile, thus the ED addition/dissociation equilibrium between [Co(acac)$_2$(ED)] and [Co(acac)$_2$(ED)$_2$] is kinetically able to stabilize the Co^{II} spin trap and thereby accelerate the polymerization by the OMRP mechanism.

To find supporting evidence for the presence of a DT process, we carried out additional polymerizations with different V-70/Co ratios. If the control mechanism were of OMRP type, the apparent rate of polymerization, k_{app}, should follow Equation (1) and thus be independent of the radical influx from the initiator. For a DT mechanism, on the other hand, the polymerization rate should follow an expression like Equation (2), for which, as in free radical polymerization, the rate of exchange k_{exch} affects only the degree of control.[3] The results of the VOAc polymerization in the presence of different amounts of V-70 are shown in Figure 9. As expected, the induction time decreases for a greater V-70 concentration, because the greater radical influx allows a faster conversion of the [Co(acac)$_2$] into the organocobalt(III) species. Figure 9 shows that the polymerization rate increases as the radical influx increases. The observed pseudo first order rate constants are $2.24\times10^{-3}\,s^{-1}$ for [V-70]/[Co^{II}]=4 and $1.04\times10^{-3}\,s^{-1}$ for [V-70]/[Co^{II}]=2. Given an estimated initiator efficiency factor of 0.6 for V-70 and the irreversible consumption of one equivalent of radicals to convert all Co^{II} to Co^{III}, the residual radical/metal ratios are 3.8 and 1.4, respectively. The ratio of the observed rate constants, $2.24\times10^{-3}/1.04\times10^{-3}=2.15$, is close to the square root of the radical concentration ratio, $(3.8/1.4)^{0.5}=1.65$. This is as expected for a DT mechanism and disagrees with an OMRP mechanism.

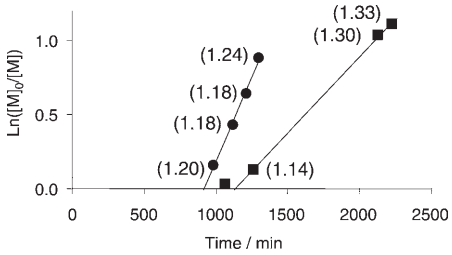

Figure 9. Semilogarithmic kinetic plots for the bulk CRP of VOAc mediated by [Co(acac)$_2$] in the presence of different amounts of V-70 at 30 °C ([VOAc]$_0$/[Co(acac)$_2$]$_0$/[ED]$_0$=500/1/30): (■) [V-70]$_0$/[Co(acac)$_2$]$_0$=2; (●)-[V-70]$_0$/[Co(acac)$_2$]$_0$=4. The values in parentheses indicate the polydispersity index of the polymer samples.

$$k_{app}=(k_p[VOAc])(k_{act}/k_{deact})[R_0(VOAc)_n\text{–}Co^{III}(acac)_2(ED)]/[Co^{II}(acac)_2(ED)] \quad (1)$$

$$k_{app}=(k_p[VOAc])(fk_d[V\text{-}70]/k_t)^{1/2} \quad (2)$$

One strong point that was previously put forward in favor of an OMRP mechanism is the fact that the isolated and purified polymer (described as a green material),[9,12] supposedly end-capped with the {–Co^{III}(acac)$_2$} fragment, can undergo chain extension upon treatment with fresh VOAc and in the absence of a new radical source.[9] This result can only be achieved for an OMRP mechanism, since the DT mechanism relies on the continuous influx of radicals from an external initiator. We have noted that the reaction mixture maintains a pale brown–pink color during the polymerization procedure, and that the polymer, when isolated and purified under rigorous air-free and dry conditions, is pink. However, the aliquots withdrawn from the reaction mixtures for the purpose of calculating the conversion and analyzing the polymer by SEC, turned green during the drying procedure in air. In addition, when the polymer was purified by dissolution in dry acetone and re-precipitation with dry heptane, it maintained its pink color, whereas when the procedure was carried out in the same manner but without using special precautions (regular acetone and in air), the polymer became green. We put forward the hypothesis that the pink organocobalt(III) dormant species, generated in the absence of ED, contains five-coordinate chain ends, [R_0(VOAc)$_n$–Co(acac)$_2$], and that contact with moist air changes the chemical structure of the chain end, causing the material to turn green. The color change may result from water binding to yield a six-coordinate chain end, [R_0(VOAc)$_n$–Co(acac)$_2$-(H_2O)], or from an oxidation process. The second possibility appears more likely, since no color change occurred when degassed water was added under an inert atmosphere. The chemical nature of this green chromophore is currently unknown and will be investigated at a later time. Since we have demonstrated that ED coordination renders the homolytic dissociation of the organocobalt(III) dormant species easier, and since the DFT calculations indicate that water is able to provide sufficient stabilization of the Co^{II} spin trap,

a polymer terminated by {–Co(acac)$_2$(H$_2$O)} chain ends would be able to undergo chain extension by the OMRP mechanism. To test this hypothesis, we isolated, under as rigorous conditions as possible, a pink poly(vinyl acetate) obtained by the V-70-initiated, [Co(acac)$_2$]-mediated polymerization in the absence of ED additives (M_n = 18800). Subsequently, this polymer was treated with additional fresh VOAc in bulk at 35 °C and without V-70. No significant polymerization took place over a period of one day (about 2 % after 1566 min, see Figure 10), while the color of the

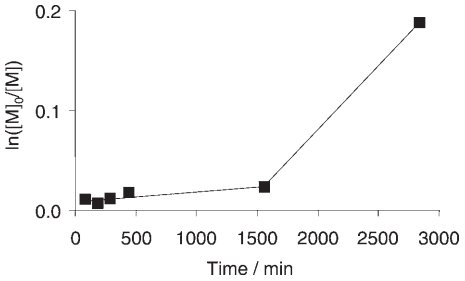

Figure 10. Semilogarithmic kinetic plots for the bulk CRP of VOAc mediated by pink [R$_0$(VOAc)$_n$–Co(acac)$_2$] (M_n = 18800) at 40 °C ([VOAc]$_0$/[Co^{III}]$_0$ = 5400:1). Water ([H$_2$O]/[Co^{III}]$_0$ = ca. 32) was added after 1566 min.

mixture remained pale pink. At this point, water was deliberately added to the reaction mixture and a faster polymerization process ensued (17 % in the subsequent 1300 min). This result demonstrates that the pink [Co^{III}(acac)$_2$]-capped dormant chain is not capable of chain extension in the absence of a fresh radical source, but does so after the addition of water. Therefore, it suggests that the previously reported[9] chain extension experiment indeed occurs through OMRP as the authors suggested, but this involves a chemically modified organocobalt(III) chain end, after exposure to moist air.

A final point of discussion is the possibility that the associative radical exchange involves an intermediate dialkylcobalt(IV) complex, lying in a local energy minimum, either higher or lower than the energy of the cobalt(III) complex (see Figure 11). If the associative species is only a transition state, characterized by one normal mode of vibration with an imaginary frequency (Figure 11a), the mechanism is that of a typical degenerative transfer and the control of polydispersity is only ensured by kinetic factors.[3] If, on the other hand, a stable intermediate dialkyl Co^{IV} species exists (Figure 11c), then we have an OMRP mechanism, the Co^{IV} complex being the depository of the dormant polymer chain. In an intermediate situation (Figure 11b) the Co^{IV} intermediate is unstable but has a certain lifetime and will help to insure better chain growth control. It should be mentioned that at least one sufficiently stable alkylcobalt(IV) complex for isolation and characterization, [Co(norbornyl)$_4$], is known, though its stability may be attributed to the severe steric encumbrance of the ligand coordination sphere.[51,52] For the present system, an aliquot of the reaction mixture did not

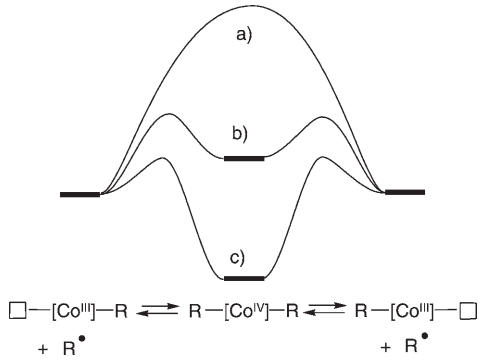

Figure 11. Possible energy profiles for the associative radical exchange on [Co^{III}(acac)$_2$]–PVOAc.

reveal any EPR signal after quenching to liquid nitrogen temperature. Thus, it seems that the dialkyl Co^{IV} species is either a transition state or an intermediate with too short a lifetime for measurement by this technique.

Conclusion

The present study has shown that the [Co(acac)$_2$]-mediated polymerization of VOAc may occur by either one of two fundamentally different mechanisms: a degenerative transfer in the absence of ligands capable of establishing strong interactions with the cobalt center, that is, when the [R$_0$-(VOAc)$_n$–Co(acac)$_2$] dormant species remains five-coordinate, and a reversible homolytic cleavage of the dormant organocobalt(III) species in the presence of strongly binding electron donors, that is, when the dormant species is six-coordinate, [R$_0$(VOAc)$_n$–Co(acac)$_2$(ED)]. The second mechanism is accelerated by more strongly binding EDs, because of the energetic stabilization of the Co^{II} spin trap due to the formation of 6-coordinate [Co(acac)$_2$(ED)$_2$]. On the other hand, no degenerative transfer is possible in the presence of ED, because the latter blocks the coordination site that is necessary for the associative radical exchange. Future efforts in our laboratories will be directed at the synthesis, isolation, and characterization of simple model complexes of the organocobalt(III) dormant chain, and to application of the ED modulation of the [Co(acac)$_2$] reactivity to the development of new polymeric architectures.

Acknowledgement

KM greatly appreciates the financial support from the National Science Foundation (DMR-0549353 and CHE-0405627), Mitsui Chemicals, Inc. and CRP Consortium at Carnegie Mellon University. RP thanks the ANR (Contract No. NT05-2_42140) and CINES and CICT (Project CALMIP) for granting free computational time.

[1] "Controlled/Living Radical Polymerization: From Synthesis to Materials": *ACS Symp. Ser.* **2006**, *944*, whole volume.

[2] K. Matyjaszewski, T. P. Davis, *Handbook of Radical Polymerization*, Wiley-Interscience, Hoboken, NJ, **2002**.
[3] A. Goto, T. Fukuda, *Prog. Polym. Sci.* **2004**, *29*, 329.
[4] C. J. Hawker, A. W. Bosman, E. Harth, *Chem. Rev.* **2001**, *101*, 3661.
[5] B. B. Wayland, G. Poszmik, S. L. Mukerjee, M. Fryd, *J. Am. Chem. Soc.* **1994**, *116*, 7943.
[6] B. B. Wayland, L. Basickes, S. Mukerjee, M. Wei, M. Fryd, *Macromolecules* **1997**, *30*, 8109.
[7] "Controlled Radical Polymerization": L. D. Arvanitopoulos, M. P. Greuel, B. M. King, A. K. Shim, H. J. Harwood, *ACS Symp. Ser.* **1998**, *685*, 316.
[8] Z. Lu, M. Fryd, B. B. Wayland, *Macromolecules* **2004**, *37*, 2686.
[9] A. Debuigne, J.-R. Caille, R. Jerome, *Angew. Chem.* **2005**, *117*, 1125; *Angew. Chem. Int. Ed.* **2005**, *44*, 1101.
[10] A. Debuigne, J.-R. Caille, C. Detrembleur, R. Jerome, *Angew. Chem.* **2005**, *117*, 3505; *Angew. Chem. Int. Ed.* **2005**, *44*, 3439.
[11] A. Debuigne, J.-R. Caille, N. Willet, R. Jerome, *Macromolecules* **2005**, *38*, 9488.
[12] A. Debuigne, J.-R. Caille, R. Jerome, *Macromolecules* **2005**, *38*, 5452.
[13] C. Detrembleur, A. Debuigne, R. Bryaskova, B. Charleux, R. Jerome, *Macromol. Rapid Commun.* **2006**, *27*, 37.
[14] R. Poli, *Angew. Chem.* **2006**, *118*, 5180; *Angew. Chem. Int. Ed.* **2006**, *45*, 5058.
[15] J.-S. Wang, K. Matyjaszewski, *J. Am. Chem. Soc.* **1995**, *117*, 5614.
[16] J.-S. Wang, K. Matyjaszewski, *Macromolecules* **1995**, *28*, 7901.
[17] T. E. Patten, J. Xia, T. Abernathy, K. Matyjaszewski, *Science* **1996**, *272*, 866.
[18] M. Kamigaito, T. Ando, M. Sawamoto, *Chem. Rev.* **2001**, *101*, 3689.
[19] K. Matyjaszewski, J. Xia, *Chem. Rev.* **2001**, *101*, 2921.
[20] S. G. Gaynor, J.-S. Wang, K. Matyjaszewski, *Macromolecules* **1995**, *28*, 8051.
[21] M. C. Iovu, K. Matyjaszewski, *Macromolecules* **2003**, *36*, 9346.
[22] S. Yamago, *J. Polym. Sci. Part A* **2006**, *44*, 1.
[23] J. Chiefari, E. Rizzardo, in *Handbook of Radical Polymerization* (Eds.: K. Matyjaszewski, T. P. Davis), Wiley-Interscience, Hoboken, NJ, **2002**, p. 629.
[24] P. Corpart, D. Charmot, T. Biadatti, S. Z. Zard, D. Michelet, in *PCT Int. Appl.,* WO9858974, Rhodia, France, **1998**.
[25] B. B. Wayland, X.-F. Fu, Z. Lu, M. Fryd, *Polym. Prepr.* **2005** (*230th ACS National Meeting*, August 28-September 1, ***2005***, Washington, DC).
[26] a) B. B. Wayland, X. Fu, C.-H. Peng, Z. Lu, M. Fryd, *ACS Symp. Ser.* **2006**, *944*, 358; b) B. B. Wayland, C.-H. Peng, X. Fu, Z. Lu, M. Fryd, *Macromolecules* **2006**, *39*, 8219.
[27] F. A. Cotton, R. H. Soderberg, *Inorg. Chem.* **1964**, *3*, 1.
[28] F. A. Cotton, R. C. Elder, *Inorg. Chem.* **1965**, *4*, 1145.
[29] J. Burgess, J. Fawcett, D. R. Russell, S. R. Gilani, *Acta Crystallogr. Sect. C* **2000**, *56*, 649.
[30] F. A. Cotton, J. S. Wood, *Inorg. Chem.* **1964**, *3*, 245.
[31] L.-C. Wang, H.-Y. Jang, Y. Roh, V. Lynch, A. J. Schultz, X. Wang, M. J. Krische, *J. Am. Chem. Soc.* **2002**, *124*, 9448.
[32] J. P. Fackler, Jr., *Inorg. Chem.* **1963**, *2*, 266.
[33] F. A. Cotton, R. C. Elder, *Inorg. Chem.* **1966**, *5*, 423.
[34] M. Doering, H. Goerls, E. Uhlig, *Z. Anorg. Allg. Chem.* **1991**, *603*, 7.
[35] G. J. Bullen, *Acta Crystallogr.* **1959**, *12*, 703.
[36] P. Werndrup, V. G. Kessler, *J. Chem. Soc. Dalton Trans.* **2001**, 574.
[37] R. C. Elder, *Inorg. Chem.* **1968**, *7*, 1117.
[38] M. Doering, W. Ludwig, E. Uhlig, S. Wocadlo, U. Mueller, *Z. Anorg. Allg. Chem.* **1992**, *611*, 61.
[39] A. D. Becke, *J. Chem. Phys.* **1993**, *98*, 5648.
[40] Gaussian 03, Revision B.04, M. J. Frisch, G. W. Trucks, H. B. Schlegel, G. E. Scuseria, M. A. Robb, J. R. Cheeseman, J. A. Montgomery, Jr., T. Vreven, K. N. Kudin, J. C. Burant, J. M. Millam, S. S. Iyengar, J. Tomasi, V. Barone, B. Mennucci, M. Cossi, G. Scalmani, N. Rega, G. A. Petersson, H. Nakatsuji, M. Hada, M. Ehara, K. Toyota, R. Fukuda, J. Hasegawa, M. Ishida, T. Nakajima, Y. Honda, O. Kitao, H. Nakai, M. Klene, X. Li, J. E. Knox, H. P. Hratchian, J. B. Cross, V. Bakken, C. Adamo, J. Jaramillo, R. Gomperts, R. E. Stratmann, O. Yazyev, A. J. Austin, R. Cammi, C. Pomelli, J. W. Ochterski, P. Y. Ayala, K. Morokuma, G. A. Voth, P. Salvador, J. J. Dannenberg, V. G. Zakrzewski, S. Dapprich, A. D. Daniels, M. C. Strain, O. Farkas, D. K. Malick, A. D. Rabuck, K. Raghavachari, J. B. Foresman, J. V. Ortiz, Q. Cui, A. G. Baboul, S. Clifford, J. Cioslowski, B. B. Stefanov, G. Liu, A. Liashenko, P. Piskorz, I. Komaromi, R. L. Martin, D. J. Fox, T. Keith, M. A. Al-Laham, C. Y. Peng, A. Nanayakkara, M. Challacombe, P. M. W. Gill, B. Johnson, W. Chen, M. W. Wong, C. Gonzalez, J. A. Pople, Gaussian, Inc., Wallingford CT, **2004**.
[41] P. J. Hay, W. R. Wadt, *J. Chem. Phys.* **1985**, *82*, 270.
[42] F. K. Shmidt, L. O. Nindakova, B. A. Shainyan, V. V. Saraev, N. N. Chipanina, V. A. Umanetz, *J. Mol. Catal. A* **2005**, *235*, 161.
[43] G. N. La Mar, W. D. Horrocks, Jr., R. H. Holm, *NMR of Paramagnetic Molecules*, Academic Press, New York, **1973**.
[44] I. Bertini, C. Luchinat, *Coord. Chem. Rev.* **1996**, *150*, 1.
[45] J. E. Huheey, E. A. Keiter, R. L. Keiter, *Inorganic Chemistry: Principles of Structure and Reactivity*, 4th ed., Harper & Row, New York, **1993**.
[46] A. P. Gulya, G. V. Novitskii, S. G. Shova, M. D. Mazus, I. Sandu, *Koord. Khim.* **1993**, *19*, 227.
[47] D. Dodd, M. D. Johnson, *J. Organomet. Chem.* **1973**, *52*, 1.
[48] J. Halpern, *Science* **1985**, *227*, 869.
[49] K. P. Jensen, U. Ryde, *J. Am. Chem. Soc.* **2005**, *127*, 9117.
[50] N. M. Beileryan, R. G. Melkonyan, O. A. Chaltykyan, *Arm. Khim. Zh.* **1971**, *24*, 203.
[51] B. K. Bower, H. G. Tennent, *J. Am. Chem. Soc.* **1972**, *94*, 2512.
[52] B. K. Bower, M. Findlay, C. W. Chien, *Inorg. Chem.* **1974**, *13*, 759.

Received: October 13, 2006
Published online: February 5, 2007

